An Efficient Approach for the Detection of Brain Tumor Using Fuzzy Logic and U-NET CNN Classification

Sarmad Maqsood[1], Robertas Damasevicius[1(✉)], and Faisal Mehmood Shah[2]

[1] Department of Software Engineering, Kaunas University of Technology, 51368 Kaunas, Lithuania
sarmad.maqsood@ktu.edu, robertas.damasevicius@ktu.lt
[2] Pakistan Space & Upper Atmosphere Research Commission, Karachi 75270, Pakistan

Abstract. Clinical diagnosis has increased marvelous significance in current day healthcare systems. This article proposes a brain tumor detection method using edge detection based fuzzy logic and U-NET Convolutional Neural Network (CNN) classification method. The proposed tumor segmentation system is based on image enhancement, fuzzy logic based edge detection, and classification. The input images are pre-processed using the contrast enhancement and fuzzy logic-based edge detection method is applied to identify the edge in the source images and dual tree-complex wavelet transform (DTCWT) is used at different scale levels. The features are calculated from the decayed sub-band images and these features are then categorized using U-NET CNN classification which recognizes the meningioma and non-meningioma brain images. The proposed method is evaluated using accuracy, sensitivity, specificity, and dice coefficient index. Simulation study demonstrates that the proposed technique achieves better performance, both visually and quantitatively in comparison with other approaches.

Keywords: Brain MRI · Medical image processing · Deep learning · Image classification · Segmentation · Fuzzy logic

1 Introduction

The enormous growth of cell areas in the brain can lead to tumors, which occur in people of all ages. Based on the area, size and location, these large tumor cells are divided into cancerous and non-cancerous cells [1]. The early stage of cancer cells is called benign and is referred to as the primary tumor area. The severe stages of cancer cells are called malignancies and secondary tumor area. Primary tumors are curable, and their growth controlled by taking the appropriate medications. The secondary tumor can be cured only if the affected patient receives adequate

© Springer Nature Switzerland AG 2021
O. Gervasi et al. (Eds.): ICCSA 2021, LNCS 12953, pp. 105–118, 2021.
https://doi.org/10.1007/978-3-030-86976-2_8

treatment with surgery or radiation [2]. Brain tumors are known to damage surrounding brain tissue, so tumor progression must be carefully assessed to extend patients survival time [3]. Magnetic resonance imaging (MRI) is determined to be one of the most common diagnostic approaches for brain tumors, and numerous MRI methods can be used to recognize the brain tumor. Each of the above MRI methods has a different relaxation time, so it can be used to recognize different brain tissues [4]. This deadly disease can be controlled early only by proper scanning the brain area at the initial stage to detect the tumor.

Due to the complexity and change in tumor structure and the similarity in intensity between tumor tissue and normal brain tissue, tumor segmentation is a difficult task. While certain tumors such as meningioma can be easily isolated, other tumors such as glioma and glioblastoma are problematic [5]. This makes manual segmentation of tumor a cumbersome task, and in some cases, due to the various appearance and vague shape of the tumor, changes in the oncologist's segmentation results may be observed. Therefore, an automatic segmentation method must be developed to facilitate this difficult task.

Meningioma is a tumor that procedures in the skull and protects the brain and the spinal cord. Specially, tumors form in a three-layered membrane called the meninges [6]. Meningiomas usually appear as extra axial lobar masses with distinct margins [11]. The existence rate of patients having meningioma is contingent on the size and location of the tumor area and the patient's age. Annexations, headaches, and limb weakness are signs of meningiomas. If caught early and treated with appropriate medical treatment, most malignant meningioma tumors can be cured. The diameter of benign meningioma tumors is approximately less than 2 mm and the diameter of malignant meningioma tumors ranges from 2 mm to 5 cm [3].

Manually identifying brain tumors and tracking their changes over time can be unvaried and error prone [6]. Since it requires an automated system to replace the traditional manual approaches. Previous methods have some limitations i.e., many traditional approaches use tagging methods to detect abnormal pixels in the brain region, existing methods cannot detect inner border pixels which are incompatible for various brain tumor detection systems. In this article, MRI is chosen as compared to computed tomography (CT) scanning because of the area enhanced by the contrast agent and its visibility, which can be well processed by various image processing methods [7]. MRI has been used to detect ischemic stroke lesions [8] and schizophrenia [9] in brain image slices. It also has been applied to detect tumour in other tissues such as breasts [10]. Therefore, numerous brain tumor detection approaches use MR imaging modalities.

The remaining paper is organized as follows. Section 2 study the notable related work on brain tumor detection. In Sect. 3 the detailed methodology of the proposed approach is discussed. Section 4 evaluates the performance of the proposed method in comparison with the other methods and, finally, Sect. 5 concludes this article with future research goals.

2 Related Work

Over the past few years, more and more work has been performed in the brain tumor segmentation field. This is determined by the significance of this topic in the medical society [3,12,13]. Different researchers have used different techniques to segment brain tumors. Currently, the deep learning based methods are considered as state-of-the-art in image-based recognition and segmentation of various cancers [14,15] and other diseases [16,17]. Khan et al. [18] uses two pre-trained CNN models (VGG19 and VGG16) for feature extraction. The best features were selected using the correntropy based joint approach and extreme learning machine (ELM) classifier is employed to classify the features. Seetha et al. [19] uses CNN for the brain tumors classification. They studied the structural variability of tumors around adjacent areas. The authors proposed a small kernel to keep the weight of each neuron small. Jasmine et al. [20] uses the adaptive neuro fuzzy inference classification technique to detect and locate tumors on MRI of the brain. The tumor areas are improved using histogram equalization technique without the detection of edges in brain images. Bansal et al. [21] used the swarm ant lion algorithm for the process of locating and detecting tumors in MRI. The method is likened with the probabilistic neural network to verify the effectiveness of the method. Devkota et al. [22] created a mathematical segmentation system of linear parameters to detect irregular tumor areas in brain images. The author derives statistical and texture characteristics of images from brain sources and divides the images into malignant or non-malignant images based on these calculated brain image characteristics. The tumor area was segmented using linear limited morphological processes. Ganeshkumar et al. [23] used the watershed segmentation technique to brain MR imaging to locate the tumor areas. The segmentation process uses a predetermined set of labeling methods, maximizing the precision of the tumor segmentation. Prasava et al. [24] presented a method to detect and recognize boundary pixels in brain images to segment tumor areas. This approach only detects the abnormal border of the tumor area but cannot detect the inner border of the tumor area. Lai et al. [25] presented a CNN method for semantic image segmentation. The authors suggest reducing the size of the convolution filter and reducing the input channels number to create the model more portable. Likewise, the author in [26] presented a lightweight CNN for real-time semantic segmentation. This method has omitted numerous connection areas to reduce the parameters of the network and rise the speed. Finally, Woźniak et al. [27] suggested a correlation learning mechanism (CLM) for deep learning models that fuses CNN with a classic neural network architecture. This support network helps the main CNN to find the most suitable filers for pooling and convolution layers, and the resulting architecture is used for brain tumor detection in CT scan images.

All the aforementioned methods achieved enhanced results, but still they exhibit several limitations such as many conventional approaches use tagging methods to detect abnormal pixels in the areas of the brain and existing approaches fail to detect the inside of the edge pixels, which is not appropriate for brain tumor detection systems.

3 The Proposed Method

The proposed approach for tumor segmentation and classification comprise of contrast enhancement, fuzzy logic-based feature extraction method, and classification. Firstly, the source brain image is pre-processed through contrast enhancement method for better visualization and then dual tree-complex wavelet transform (DTCWT) is employed to the improved image at different scale levels. Afterwards, the fuzzy-logic based feature extraction approach is used to find the edges. U-NET CNN is employed for the detection and classification of brain tumor imaging. The proposed framework contains two different modules: up sampling and the down sampling. The proposed U-NET CNN framework uses the perception of zero padding in both up sampling and down sampling to enhance the response of each layer. Figure 1 illustrates the workflow of brain tumor detection and classification.

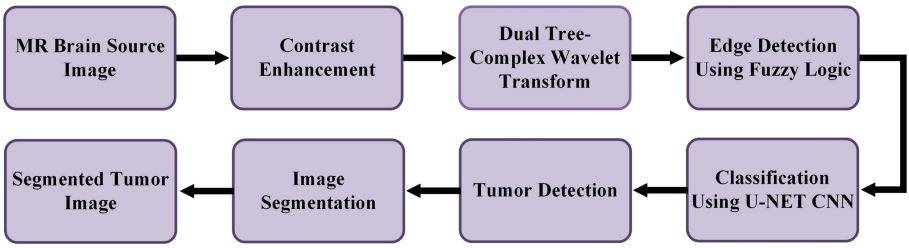

Fig. 1. Schematic diagram of the proposed system for brain tumor segmentation.

3.1 Pre-processing

To intensify the low contrast images the histogram equalization approach seems to be a more effective technique. Non-parametric modified histogram equalization (NPMHE) [30] is applied to increase the contrast and keep the average brightness of the source image.

Firstly, NMHE removes the spikes from the original histogram. After that the process clipped the histogram and computed the cumulative distribution function of the transitional rehabilitated histogram from the uniform one. After that it works as a weighting factor to create a final updated histogram. Equation (1) regulates a threshold and the pixels higher than the threshold contribute in the modified histogram as,

$$W_c(j) = r[j \mid H], \tag{1}$$

where $r[j \mid H]$ is the occurrence probability of ith intensity-level given the horizontal contrast variation H. A measure of un-equalization (ζ_u) is calculated as in Eq. (2).

$$\zeta_u = sum(u - \varsigma_c v). \tag{2}$$

The value of ζ_u is a pointer to those images which does not follow a uniform distribution. u is a uniform probability density function and $\varsigma_c v$ is a modified clipped histogram designed from the original histogram. The weighted factor of the modified PDF is given in Eq. (3).

$$\vartheta_F = (\varsigma_c v)W_c + (1 - \zeta_u)u. \tag{3}$$

The CDF of the image is attained from the reformed histogram ϑ_F in Eq. (4).

$$t_D(n) = \sum_{j=0}^{n} \vartheta_F(n). \tag{4}$$

The transformation operation $S(c)$ attained by using t_D given in Eq. (5).

$$S(c) = [(\alpha - 1)t_D(n) + \frac{1}{2}], \tag{5}$$

where $S(c)$ is used to obtain the contrast enhanced images. Contrast enhancement results improved the edges in the input images.

Figure 2 shows the enhancement from source brain images. From the image, it can be observed that after applying the enhancement method, the gradients of the image are enhanced keeping the information of the source image.

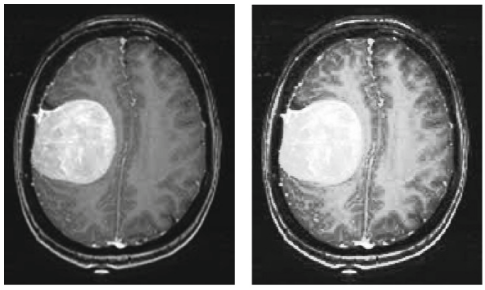

(a) (b)

Fig. 2. Contrast enhancement result. (a) Source brain MRI, (b) Contrast enhanced image.

3.2 Dual-Tree Complex Wavelet Transform

This transform is employed to alter spatial resolution pixel to multi resolution pixel. The Discrete Wavelet Transform (DWT) is employed as a traditional decomposition technique for acquiring sub band images of numerous scales. DWT has a limit on offset variation, which affects the resolution factor at different zoom levels. This limitation can be overcome by using DTCWT to capture a broken

sub band image. The DTCWT framework is intended with complex wavelet and complex scaling functions. The advantage of DTCWT is that it can extract edges from detail subbands, which are abundant in brain tissues. Those edges serve as discriminant features between diseased brain and healthy brain tissues [28].

The DTCWT operation is given in Eq. (6) as:

$$\psi(s) = \psi_r(s) + j\psi_{imj}(s) \tag{6}$$

The complex wavelet function having real and imaginary parts is expressed by Eqs. (7) and (8).

$$\psi_r(s) = \sqrt{2} \times \sum Q_r(s) \times \psi_r(2s - g) \tag{7}$$

$$\psi_{imj}(s) = \sqrt{2} \times \sum Q_{imj}(s) \times \psi_{imj}(2s - g) \tag{8}$$

The proposed method uses four levels of DTCWT to obtain the decomposed sub band images.

3.3 Feature Extraction

Fuzzy logic previously has been employed successfully for detection of edges in complex medical images such as retinal images [29]. Here, a fuzzy logic-based edge detection approach is presented to acquire the edges map of the contrast enhanced image. The workflow of the proposed fuzzy edge detection method is displayed in Fig. 3. A 3×3 convolution mask is created to obtain the grayscale neighborhood pixels values in the contrast enhanced image. The grayscale neighborhood pixels values acquired from the mask are preprocessed before the fuzzy inference system. The system is created to seize the processed values as the input. Then convert these values to a fuzzy plane. A library of fuzzy rules has been determined and displays the edge pixels of the output image. The output of the system is computed using the centroid technique and defuzzification according to the Mamdani's inference.

Firstly, a 3×3 convolution mask is created using the patterns shown in Fig. 4. These 16 fuzzy patterns represent a variety of possible boundary shapes. Select a pattern that mimics the type and orientation of edges that may appear. Patterns are examples of edges. The 'u', 'v', and 0 represent pixels in the edge model. The values $u = 0.5$ and $v = 1.2$ have been selected experimentally in this work. These values are fixed in all images. A recognizable addition is that increasing the number of models to 16 and above does not significantly improve the edge results. If the number of models is reduced, many edges are lost.

With 16 patterns all the edges are detected. After that, hesitation level or Intuitionistic Fuzzy Index (IFI) is found in Eq. (9).

$$IFI = \chi \times (1 - \psi(s)). \tag{9}$$

It calculates the Intuitionistic Fuzzy Divergence (IFD) between each element of the pattern, the size of the image window is the same as the pattern, and the

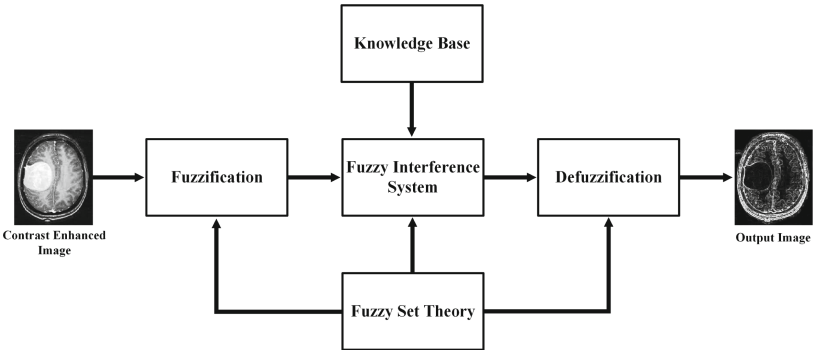

Fig. 3. Schematic diagram of the fuzzy logic-based edge detection method.

$$\begin{vmatrix} 0 & v & u \\ 0 & v & u \\ 0 & v & u \end{vmatrix} \begin{vmatrix} u & u & u \\ 0 & 0 & 0 \\ v & v & v \end{vmatrix} \begin{vmatrix} u & u & v \\ u & v & 0 \\ v & 0 & 0 \end{vmatrix} \begin{vmatrix} v & v & v \\ 0 & 0 & 0 \\ u & u & u \end{vmatrix}$$

$$\begin{vmatrix} u & u & u \\ v & v & v \\ 0 & 0 & 0 \end{vmatrix} \begin{vmatrix} u & v & 0 \\ u & v & 0 \\ u & v & 0 \end{vmatrix} \begin{vmatrix} 0 & 0 & 0 \\ u & u & u \\ v & v & v \end{vmatrix} \begin{vmatrix} v & u & u \\ 0 & v & u \\ 0 & 0 & v \end{vmatrix}$$

$$\begin{vmatrix} v & u & 0 \\ v & u & 0 \\ v & u & 0 \end{vmatrix} \begin{vmatrix} u & 0 & v \\ u & 0 & v \\ u & 0 & v \end{vmatrix} \begin{vmatrix} 0 & 0 & 0 \\ v & v & v \\ u & u & u \end{vmatrix} \begin{vmatrix} o & u & v \\ 0 & u & v \\ 0 & u & v \end{vmatrix}$$

$$\begin{vmatrix} v & v & v \\ u & u & u \\ 0 & 0 & 0 \end{vmatrix} \begin{vmatrix} v & 0 & u \\ v & 0 & u \\ v & 0 & u \end{vmatrix} \begin{vmatrix} v & 0 & 0 \\ u & v & 0 \\ u & u & v \end{vmatrix} \begin{vmatrix} 0 & 0 & v \\ 0 & v & u \\ v & u & u \end{vmatrix}$$

Fig. 4. Edge detection using 16 patterns.

maximum-minimum correlation of the equation is used to select the minimum IFD value in Eq. (10) as:

$$IFD(u, v) = Maxnumber[min(IFD(U, v))]. \tag{10}$$

The highest consequence is placed at the centered point in the image. Then, from the fuzzy domain matrix the edge images are transformed into the pixel images in the interval (1–255) $\times$ 255 and after setting the threshold and applying the morphological operations the final image is obtained.

3.4 U-NET Based CNN Classification

The U-NET CNN is employed for brain tumor imaging detection and classification. The proposed framework contains two different elements: up sampling and down sampling. The down sampling component of the proposed U-NET

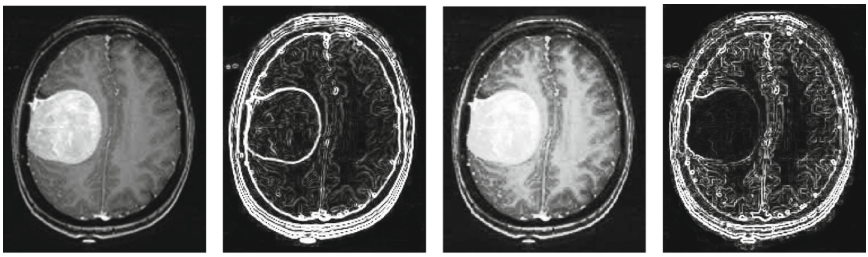

(a) (b) (c) (d)

Fig. 5. Edge detection results. (a) Source brain MRI, (b) Gradient of (a) using fuzzy edge detection, (c) Contrast enhancement using NMHE [30], and (d) Gradient of (c) using fuzzy edge detection.

CNN framework contains six convolution sub-modules, and each convolution sub-module has three convolution layers. Every convolutional layer contains 32 filters with a 3×3 window size. The MRI of the brain of origin passes through each convolutional layer and generates posterior internal features. The size of the inner convolution function is important. To decrease the size of the internal features made by the convolution layer, a pooling layer is employed after the convolution submodule. The pooling layer is divided into averaging and maximum pooling. Average pooling locates a 3×3 mask on the inner feature set and then choose the mean of feature values as the final response from the pooling layer. Maximum pooling locates a 3×3 mask on the internal feature set and choose the maximum value of the feature values as the final response from the pooling layer. Therefore, by applying the proposed framework with maximum pooling, loss of functional value can be avoided. Unlike the inconsistent flow, the extended flow consists of sampling the feature map and immediately following it with a 2×2 size convolution. After concatenation, the convolution operation is applied on the two 3×3 kernels and ReLU is activated. Finally, by applying a 1×1 convolution to the last layer, a vector of each 56 component is assigned to the desired class (Fig. 5).

The proposed U-NET CNN operates the perception of zero padding for both up and down sampling to enhance the response of each layer that is not existing in the usual U-NET. Figure 6 shows the architecture of U-NET CNN. Figure 7 shows the benign and malignant meningioma brain images and Fig. 8 displayed the benign and malignant non-meningioma brain images. To segment out the tumor area the morphological gradient function is calculated using Eq. (11).

$$\phi(I(r,s)) = (I(r,s) \oplus D) - (I(r,s) \ominus D), \tag{11}$$

where $I(r,s) \oplus D$ denotes the elementary dilation function and $I(r,s) \ominus D$ denotes the elementary erosion function.

The gradients are computed using the Eq. (12).

$$\Delta(I(r,s)) = (I(r,s) \oplus D) - 2 \times I(r,s) + (I(r,s) \ominus D), \tag{12}$$

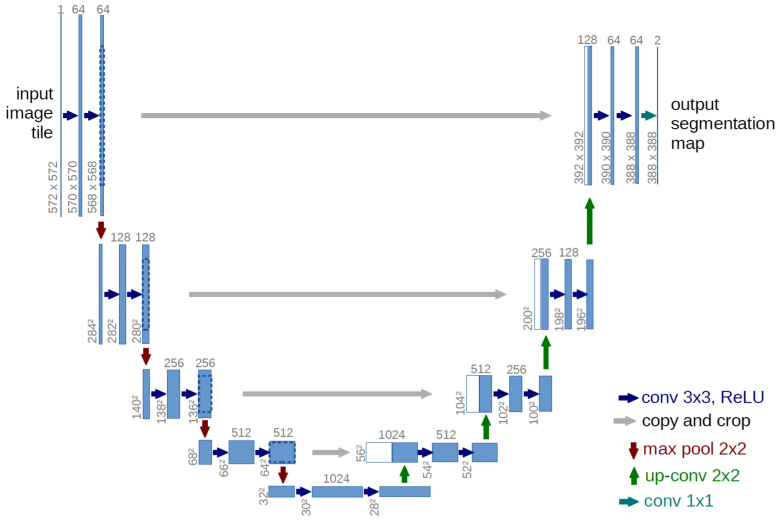

Fig. 6. U-NET CNN framework.

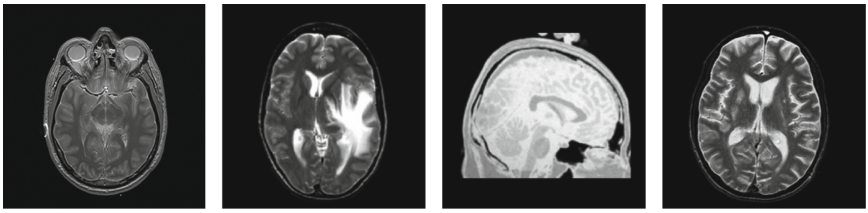

Fig. 7. Non-meningioma benign and malignant brain images.

The tumor detection and segmentation of the brain image is shown in Fig. 9.

4 Simulation Setup

The implementation of the proposed technique is performed on a laptop having Intel(R) Core (TM) i7-9750H processor, 16 GB RAM, and one NVIDIA GTX 1650 GPU with 4 GB RAM in MATLAB environment. The experiments are evaluated on meningioma brain MR images. The dataset for the brain tumor detection is acquired from [31]. The dataset includes benign and malignant brain images containing a total of 708 brain MRI. The group of 571 meningioma brain MRI, 57 glioma brain MRI, and 80 pituitary brain MRI are available. This work contains a total of 571 meningioma brain MR images. To assess the performance of the proposed brain tumor detection and segmentation technique is employed on these images.

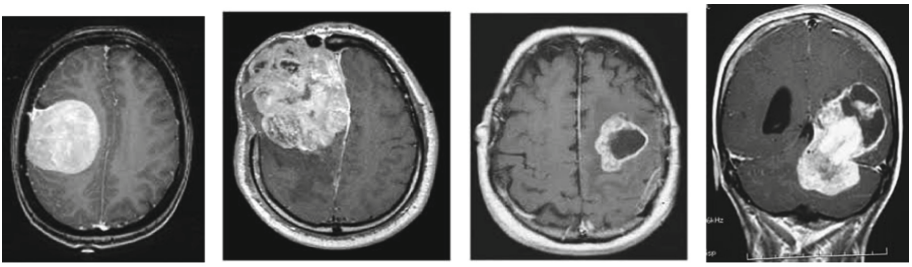

Fig. 8. Meningioma benign and malignant brain images.



Fig. 9. Meningioma brain image. (a) Source image, (b) Tumor segmented image, and (c) Tumor extraction.

4.1 Results and Discussions

The Accuracy (Ac), Sensitivity (Sn), Specificity (Sp), and Dice coefficient index (DCI) metrics are used to estimate the performance of the proposed method. The highest value of these metrics presents better performance. These metrics are defined as follows.

$$Ac = \frac{K_{TP} + K_{TN}}{K_{TP} + K_{TN} + K_{FN} + K_{FP}} \times 100\% \tag{13}$$

$$Sn = \frac{K_{TP}}{K_{TP} + K_{FN}} \times 100\% \tag{14}$$

$$Sp = \frac{K_{TN}}{K_{TN} + K_{FP}} \times 100\% \tag{15}$$

$$DCI = \frac{2 \times K_{TP}}{2 \times K_{TP} + K_{FN} + K_{FP}} \times 100\% \tag{16}$$

where K_{TP} denotes the true positive, K_{TN} denotes the true negative, K_{FN} denotes the false negative, and K_{FP} denotes the false positive.

Table 1 demonstrates the simulation results of the proposed technique using the U-NET CNN classification method. The proposed system attains the Ac of

98.45%, Sn of 98.04%, Sp of 98.86%, and DCI of 96.95%. From Table 2, note that the proposed system for detecting the brain tumor using the U-NET CNN classifier attains better performance.

Table 1. Quantitative evaluation of the proposed approach using U-NET CNN.

Proposed method	
Parameters	U-NET CNN classification method (%)
Accuracy (Ac)	98.45
Sensitivity (Sn)	98.04
Specificity (Sp)	98.86
Dice coefficient index (DCI)	96.95
Classification accuracy (CAc)	98.59

Table 2 evaluates the proposed brain tumor detection system with other latest methods in terms of classification accuracy. Using the same dataset and the same number of meningioma brain MRIs, all methods were compared, and performance was evaluated quantitatively. The U-NET CNN classification method was used for brain tumor detection and segmentation, and 571 MRI of meningioma correctly classified 563 brain images of meningioma, and the classification accuracy rate reached 98.59%. From Table 2, it can be concluded that the proposed system has better accuracy of classification than other advanced methods. The performance of the proposed system is also determined using the receiver operating characteristic (ROC) curve and confusion matrix. The ROC curve and confusion matrix of the proposed U-NET CNN classification method are illustrated in Fig. 10.

Table 2. Performance comparison with other state-of-the-art approaches.

Authors	Methods	Classification accuracy (%)
Tripathi et al. [32]	Support Vector Machine (SVM)	94.63
Cheng et al. [33]	Linear discriminant analysis (LDA)	93.60
Badza et al. [34]	CNN classification	96.50
Proposed Method	U-NET CNN classification	**98.59**

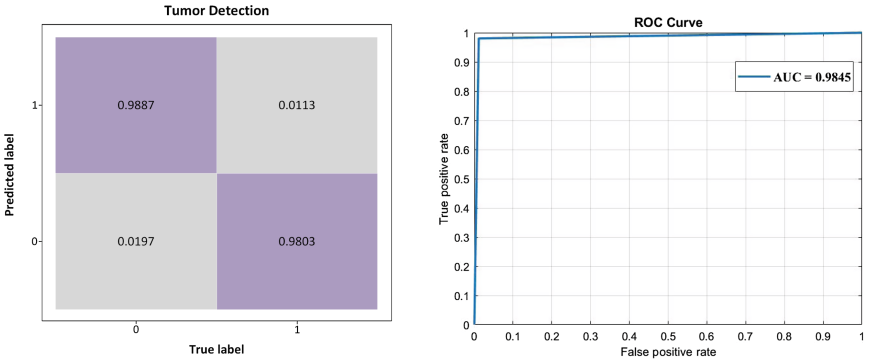

(a) Confusion Matrix (b) ROC Curve

Fig. 10. Confusion matrix and ROC curve of U-NET CNN method.

5 Conclusion

Medical imaging has increased a solid status in modern day healthcare systems. This method proposes a brain tumor segmentation method using fuzzy edge detection and U-NET CNN classification method. This method uses a contrast stretching as a processing step to enhance the edge details in an image. A 4-level DTCWT is used to decompose the MR enhanced images into subband images. Edge detection methods based on fuzzy logic are used to find edge details on MR brain images. The proposed brain tumor detection method is evaluated by applying the proposed U-NET CNN framework. Simulation results prove that the proposed approach achieves better performance, in terms of both visually and enhanced information extraction when compared to other advanced techniques. The proposed classification method for brain tumor detection attains an accuracy of 98.59%. In future, the proposed method will further be analyzed for other application areas of biomedical image processing such as breast cancer recognition.

References

1. Bauer, S., May, C., Dionysiou, D., Stamatakos, G., Buchler, P., Reyes, M.: Multiscale modeling for image analysis of brain tumor studies. IEEE Trans. Biomed. Eng. **59**(1), 25–29 (2011)
2. Toğaçar, M., Ergen, B., Cömert, Z.: BrainMRNet: brain tumor detection using magnetic resonance images with a novel convolutional neural network model. Med. Hypotheses **134**, 109531 (2020)
3. Havaei, M., et al.: Brain tumor segmentation with deep neural networks. Med. Image Anal. **35**, 18–31 (2017)
4. Pereira, S., Pinto, A., Alves, V., Silva, C.A.: Brain tumor segmentation using convolutional neural networks in MRI images. IEEE Trans. Med. Imaging **35**(5), 1240–1251 (2016)

5. Ohgaki, H., Kleihues, P.: Population-based studies on incidence, survival rates, and genetic alterations in astrocytic and oligodendroglial gliomas. J. Neuropathol. Exp. Neurol. **64**(6), 479–489 (2005)
6. Jansson, D., et al.: Cardiac glycosides target barrier inflammation of the vasculature, meninges and choroid plexus. Commun. Biol. **4**(1), 1–17 (2021)
7. Ke, Q., Zhang, J., Wei, W., Damaševičius, R., Woźniak, M.: Adaptive independent subspace analysis of brain magnetic resonance imaging data. IEEE Access **7**, 12252–12261 (2019)
8. Kadry, S., Damasevicius, R., Taniar, D., Rajinikanth, V., Lawal, I.A.: U-Net supported segmentation of ischemic-stroke-lesion from brain MRI slices. In: 2021 Seventh International conference on Bio Signals, Images, and Instrumentation (ICBSII) (2021). https://doi.org/10.1109/icbsii51839.2021.9445126
9. Kadry, S., Taniar, D., Damasevicius, R., Rajinikanth, V.: Automated detection of schizophrenia from brain MRI slices using optimized deep-features. In: 2021 Seventh International conference on Bio Signals, Images, and Instrumentation (ICBSII) (2021). https://doi.org/10.1109/icbsii51839.2021.9445133
10. Kadry, S., Damasevicius, R., Taniar, D., Rajinikanth, V., Lawal, I.A.: Extraction of tumour in breast MRI using joint thresholding and segmentation - a study. In: 2021 Seventh International conference on Bio Signals, Images, and Instrumentation (ICBSII) (2021). https://doi.org/10.1109/icbsii51839.2021.9445152
11. Ostrom, T.Q., et al.: CBTRUS statistical report: primary brain and other central nervous system tumors diagnosed in the United States in 2010–2014. Neuro-oncology (2017)
12. Muzammil, S.R., Maqsood, S., Haider, S., Damaševičius, R.: CSID: a novel multimodal image fusion algorithm for enhanced clinical diagnosis. Diagnostics **10**(11), 904 (2020)
13. Maqsood, S., Javed, U., Riaz, M.M., Muzammil, M., Muhammad, F., Kim, S.: Multiscale image matting based multi-focus image fusion technique. Electronics **9**(2), 472 (2020)
14. Lahoura, V., et al.: Cloud computing-based framework for breast cancer diagnosis using extreme learning machine. Diagnostics **11**(2), 241 (2021)
15. Khan, M.A., Sharif, M., Akram, T., Damaševičius, R., Maskeliūnas, R.: Skin lesion segmentation and multiclass classification using deep learning features and improved moth flame optimization. Diagnostics **11**(5), 811 (2021)
16. Akram, T., et al.: A novel framework for rapid diagnosis of COVID-19 on computed tomography scans. Pattern Anal. Appl. (2021). https://doi.org/10.1007/s10044-020-00950-0
17. Sahlol, A.T., Elaziz, M.A., Jamal, A.T., Damaševičius, R., Hassan, O.F.: A novel method for detection of tuberculosis in chest radiographs using artificial ecosystem-based optimisation of deep neural network features. Symmetry **12**(7), 1146 (2020)
18. Khan, M.A., et al.: Multimodal brain tumor classification using deep learning and robust feature selection: a machine learning application for radiologists. Diagnostics **10**(8), 565 (2020)
19. Seetha, J., Raja, S.S.: Brain tumor classification using convolutional neural networks. Biochem. Pharmacol. J. **11**(3), 1487 (2018)
20. Johnpeter, J.H., Ponnuchamy, T.: Computer aided automated detection and classification of brain tumors using CANFIS classification method. Int. J. Imaging Syst. Technol. **29**(4), 431–438 (2019)
21. Bansal, S., Kaur, S., Kaur, N.: Enhancement in brain image segmentation using swarm ant lion algorithm. IJITEE **8**(10), 1623–1628 (2019)

22. Devkota, B., Alsadoon, A., Prasad, P.W.C., Singh, A.K., Elchouemi, A.: Image segmentation for early stage brain tumor detection using mathematical morphological reconstruction. Procedia Comput. Sci. **125**, 115–123 (2018)
23. Shanthakumar, P., Ganesh Kumar, P.: Computer aided brain tumor detection system using watershed segmentation techniques. J. Imaging Syst. Technol. **25**(4), 297–301 (2015)
24. Prastawa, M., Bullitt, E., Ho, S., Gerig, G.: A brain tumor segmentation framework based on outlier detection. Med. Image Anal. **8**(3), 275–283 (2004)
25. Lai, D., Deng, Y., Chen, L.: Deepsqueezenet-CRF: a lightweight deep model for semantic image segmentation. In: 2019 International Joint Conference on Neural Networks (IJCNN), pp. 1–8 (2019)
26. Liu, J., Zhou, Q., Qiang, Y., Kang, B., Wu, X., Zheng, B.: FDDWNet: a lightweight convolutional neural network for real-time semantic segmentation. In: IEEE International Conference on Acoustics, Speech and Signal Processing (ICASSP), pp. 2373–2377 (2020)
27. Woźniak, M., Siłka, J., Wieczorek, M.: Deep neural network correlation learning mechanism for CT brain tumor detection. Neural Comput. Appl. (2021). https://doi.org/10.1007/s00521-021-05841-x
28. Wang, S., Lu, S., Dong, Z., Yang, J., Yang, M., Zhang, Y.: Dual-tree complex wavelet transform and twin support vector machine for pathological brain detection. Appl. Sci. **6**(6), 169 (2016)
29. Orujov, F., Maskeliūnas, R., Damaševičius, R., Wei, W.: Fuzzy based image edge detection algorithm for blood vessel detection in retinal images. Appl. Soft Comput. **94**, 106452 (2020)
30. Poddar, S., Tewary, S., Sharma, D., Karar, V., Ghosh, A., Pal, S.K.: Non-parametric modified histogram equalisation for contrast enhancement. IET Image Proc. **7**, 641–652 (2013)
31. Cheng, J.: Brain tumor dataset. Nanfang Hospital and General Hospital, Tianjin Medical University, China (2017). https://doi.org/10.6084/m9.figshare.1512427.v5
32. Tripathi, P.C., Bag, S.: Non-invasively grading of brain tumor through noise robust textural and intensity based features. In: Das, A.K., Nayak, J., Naik, B., Pati, S.K., Pelusi, D. (eds.) Computational Intelligence in Pattern Recognition. AISC, vol. 999, pp. 531–539. Springer, Singapore (2020). https://doi.org/10.1007/978-981-13-9042-5_45
33. Cheng, J., et al.: Enhanced performance of brain tumor classification via tumor region augmentation and partition. PLoS ONE **10**(10), e0140381 (2015)
34. Badza, M.M., Barjaktarovic, M.C.: Classification of brain tumors from MRI images using a convolutional neural network. Appl. Sci. **10**(6), 1999 (2020)